A Solution-Processable Dissymmetric Porous Organic Cage

A. G. Slater,[a*] M. A. Little,[a] M. E. Briggs,[a] K. E. Jelfs,[b] A. I. Cooper[a]

[a]Department of Chemistry and Materials Innovation Factory, University of Liverpool, Crown Street, Liverpool, L69 7ZD. Email: anna.slater@liverpool.ac.uk
[b]Department of Chemistry, Imperial College London, South Kensington, London SW7 2AZ

Abstract

Two dissymmetric racemic analogues of the chiral porous organic cage, **CC3**, were isolated and unambiguously characterised as a racemate pair of the *R,R,R,S,S,S* and *S,S,S,R,R,R*-diastereomers (**CC3**-*RS* and **CC3**-*SR*). **CC3**-*RS*/**CC3**-*SR* equals the highest porosity measured for **CC3** but is an order of magnitude more soluble, making it an excellent candidate for incorporation into a membrane for separation applications.

Introduction

The separation of chemicals and gases from crude mixtures accounts for 10–15% of the world's energy consumption, chiefly due to distillation processes.[1] Membrane-based separations can use up to 90% less energy than distillation,[2] and hence there is a demand for new materials that can be processed into separation membranes. Molecular cage compounds[3, 4] are attractive materials for membrane applications, in part due to their solution processability, which can be used to tune their porosity by crystal engineering,[5] to deposit them onto a range of substrates, and to blend them with other materials, such as polymers, to form mixed matrix membranes.[6] The porous organic cage (POC) **CC3**[7] shows remarkable hydrolytic stability and can separate noble gases,[4] SF_6 from N_2,[8] hexane[9] and xylene isomers,[10] and racemic alcohols and amines.[4, 7, 9] To date, **CC3** is the subject of more than 20 publications.

CC3 is a chiral imine cage and is synthesised from 1,3,5-triformylbenzene (TFB) and either *R,R*- or *S,S*-cyclohexanediamine (CHDA), resulting in **CC3**-*R* or -*S,* respectively. The sorption and separation capabilities of **CC3** in a chiral crystalline form arises from the window-to-window packing of the cages in the structure, which affords a diamondoid pore network, **CC3**-α, with a narrow pore size distribution (static pore diameter = 3.6 Å).[4] The pore topology found in chirally pure **CC3** (**CC3**-*R* or **CC3**-*S*) is also found in its racemate, **CC3**-*R*/**CC3**-*S*.[†] The latter racemate precipitates immediately when a solution of **CC3**-*R* is mixed with a solution of **CC3**-*S* (**Fig 1**).[11] Previous gas phase density functional theory (DFT) dimer calculations showed that heterochiral dimer pairs were more stable than homochiral dimer pairs (-169 kJ mol^{-1} versus -150 kJ mol^{-1}), explaining the rapid precipitation of a stable network on the mixing of enantiomers in solution.[11] The marked solid state stabilization of the racemic crystalline **CC3-***R*/**CC3-***S* material with respect to homochiral **CC3** was also demonstrated by crystal structure prediction.[12] More generally, this chiral window pairing extends to a range of other [4+6] tetrahedral imine POCs,[11, 13, 14] and also to non-tetrahedral POCs bearing the same chiral windows, such as linear, tubular POCs.[15]

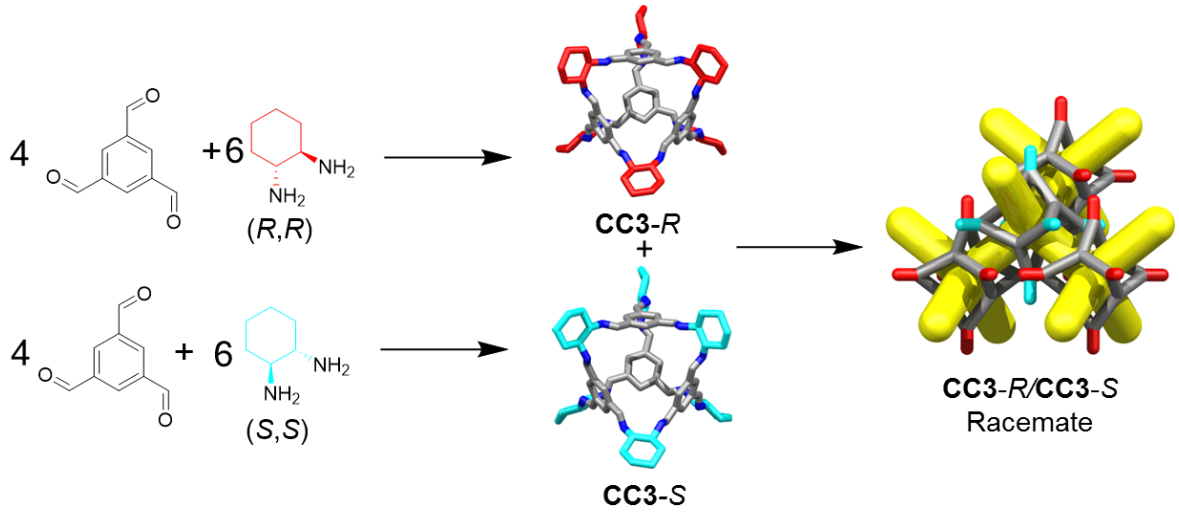

Fig 1. Reaction scheme for formation of **CC3**-*R* and **CC3**-*S*, which co-crystallises immediately upon mixing to form the racemate **CC3**-*R*/**CC3**-*S*. For **CC3**-*R*, the cyclohexane groups are shown in red; for **CC3**-*S*, in turquoise; other C, grey; N, blue; H omitted. The structure on the right is a schematic representation of the desolvated racemic **CC3**-*R*/**CC3**-*S* co-crystal; diamondoid pore network shown in yellow, simplified cage frame in grey, simplified cyclohexyl vertices in red (-*R*) and turquoise (-*S*).

CC3 and its racemate have good hydrolytic stability[16] and aminal derivatives of this POC are even stable to strong acids and bases.[17] However, for **CC3** or similar materials to find use in industrial applications, the synthesis must also be cost-efficient. Enantiomerically pure CHDA is much more expensive than racemic CHDA (£214.50 for 5 g and £12.90 for 10 mL respectively; prices obtained from Sigma-Aldrich®)[18] and hence the use of the racemic diamine would provide a significant cost benefit. The racemic POC **CC3**-*R*/**CC3**-*S* can be accessed by directly reacting TFB with (±)-*trans*-1,2-cyclohexanediamine (*rac*-CHDA)[19] and we thus sought to synthesise a porous solid in this manner (Fig. 1). The racemic co-crystal was found to precipitate rapidly from the reaction solution as a poorly-soluble crystalline solid (408 mg isolated, 47% yield, **SI Section 2.1**; **Fig 4bii** for PXRD) — a clear disadvantage for further processing, such as incorporation into membranes. Others have reported the isolation of new stereoisomers of **CC3** by collecting the precipitate resulting from the reaction of racemic CHDA with TFB.[12] In our experiments, we only observed **CC3**-*R*/**CC3**-*S* precipitating from solution (characterised by PXRD, **Fig. 4bi** and **ii**). However, analysis of the supernatant revealed the presence of two previously unreported diastereomers of **CC3**, **CC3**-*RS* and **CC3**-*SR*† (**Fig. 2**; 312 mg isolated, 36% yield, **SI Section 2.1**): that is, an asymmetric racemic cage that, unlike **CC3**-*R*/**CC3**-*S*, retains its solution processability.

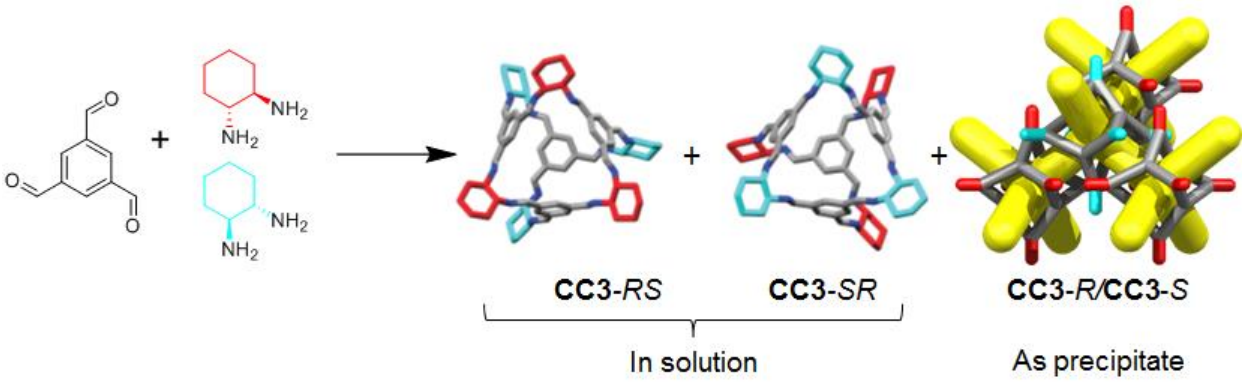

Fig 2. TFB and *rac*-CHDA react to form **CC3**-*RS* and **CC3**-*SR*, which are soluble and remain in solution, as well as **CC3**-*R* and **CC3**-*S*, which immediately co-crystallise to form the racemate, **CC3**-*R*/**CC3**-*S*, as a white precipitate. Colours as in Fig. 1.

NMR analysis (**Fig. 3, SI section 2.1.1 and 2.4**) suggested that both enantiomers, **CC3**-*RS* and **CC3**-*SR,* contain three *R*,*R*-CHDA vertices and three *S*,*S*-CHDA vertices, and that these cages were the majority enantiomers present in solution. The NMR spectra of the asymmetric species, **CC3**-*RS* and **CC3**-*SR*, are markedly different to homochiral **CC3**, which enables identification of the two cage geometries. To probe this in more detail and to ascertain if any other species were formed, even transiently, the reaction between TFB and *rac*-CHDA was analysed by ^{1}H NMR immediately after mixing, and then at 1, 2, 4, and 24 hours (**Fig. 3**). A solid precipitate formed over the course of the reaction, which was identified by PXRD analysis as the known racemate, **CC3**-*R*/**CC3**-*S* (**Fig 4bii**, red line). NMR analysis of the solution after 1 hour indicated a complex mixture of products that could not be identified unambiguously (**Fig. 3** and **SI Fig S3-4**). After 24 hours, an imine-containing cage-like product was the major component remaining in solution.

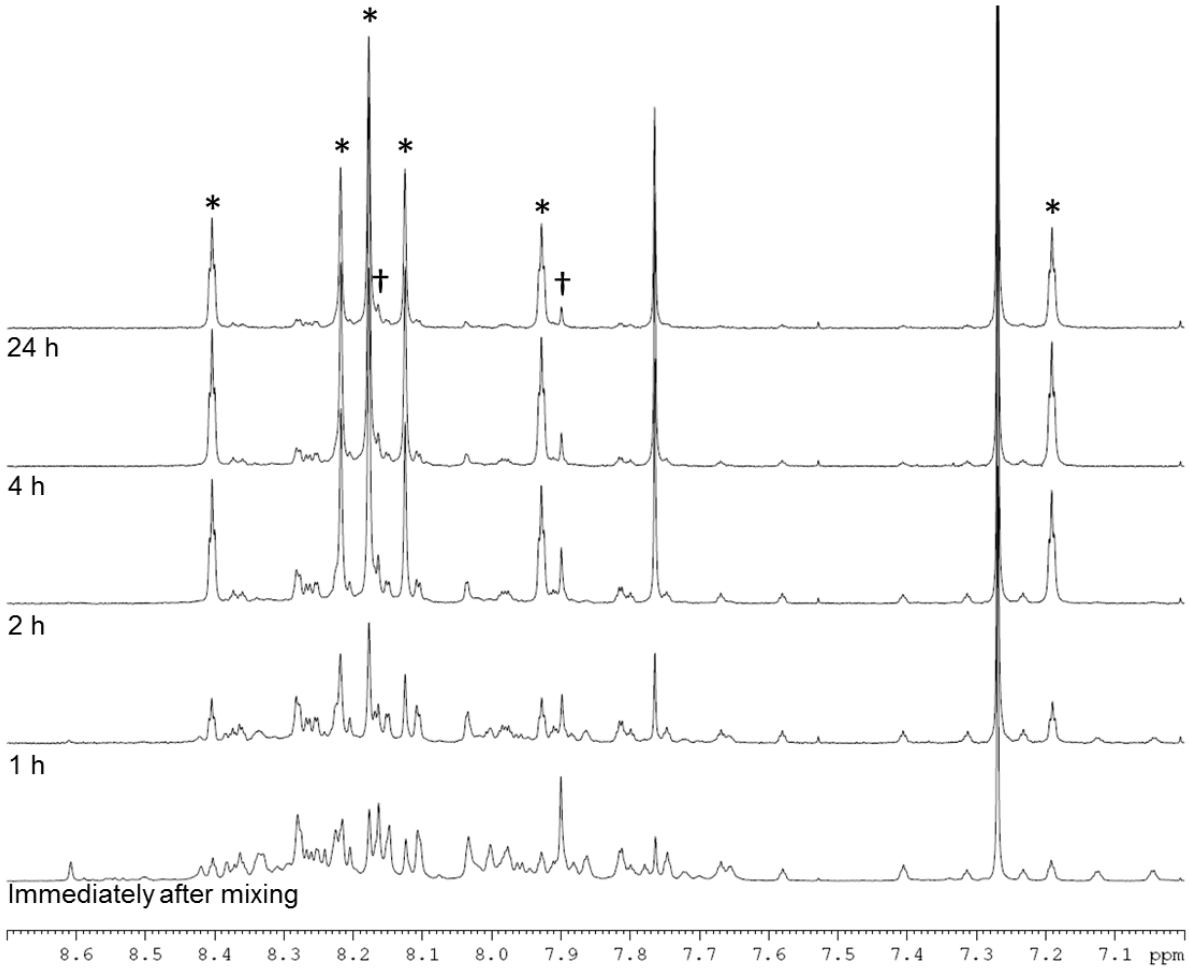

Fig. 3 NMR spectrum between 7.0 and 8.7 ppm of the reaction of TFB + *rac*-CHDA immediately after mixing, and after 1, 2, 4, and 24 hours. Asterisks indicate peaks arising from **CC3**-*RS* and **CC3**-*SR,* confirmed by 2D NMR, MS, and analysis of pure cage sample (**SI section 2**); daggers indicate peaks assigned to **CC3**-*R*- or -*S*.

We have shown previously that the reaction of TFB with a mixture of diamines, such as a binary mixture of cyclohexyldiamine and ethylene diamine, results in the formation of a statistical mixture of scrambled cage products.[20] In that example, 12 mixed cage products were formed. By contrast, only four of the possible 12 products were isolated in these experiments: **CC3**-*R*, **CC3**-*S*, **CC3**-*RS*, and **CC3**-*SR*.

DFT calculations were carried out to assess the relative stabilities of the two isomers (**SI section 3**). **CC3**-*RS* was calculated to be 10 kJ mol^{-1} less stable than **CC3**-*R*. As previously reported,[11] precipitation of the **CC3**-*R*/**CC3**-*S* co-crystal (**Fig 1**) provides an additional solid state stabilization. That **CC3**-*R*/**CC3**-*S* is not the only product suggests that both **CC3**-*RS* and **CC3**-*SR* are kinetically trapped in this configuration, and that the process is insufficiently dynamic, potentially due to the evaporation of catalytic TFA.

To explore whether the presence of **CC3**-*RS* and **CC3**-*SR* over other possible enantiomers of **CC3** was a result of the 1:1 ratio of *R,R*- and *S,S*-CHDA, reactions were performed with varying proportions of each enantiomer of CHDA (5:1, 4:2, 2:4, and 1:5 of *R,R*-CHDA:*S,S*-CHDA respectively; each set repeated twice; **SI section 2.2** and **Figs S5-6**). After 24 hours, all reactions resulted in either mixtures of homochiral **CC3** and **CC3**-*RS*/**CC3**-*SR*, or, in one

case, homochiral **CC3**, **CC3**-*RS* and -*SR*, and aldehyde starting materials. This strongly suggests that homochiral **CC3** and **CC3**-*RS*/**CC3**-*SR* are more stable than other potential diastereomers such as, for example, a cage containing 1 *S,S*-CHDA and 5 *R,R*-CHDA vertices. Such chiral self-sorting has been reported recently in salicylimine cages;[21] in that case, both products could be retained in solution in certain solvents, thus allowing a detailed analysis of their relative energies. Such analysis is not possible in our system due to the very low solubility (< 1 mg/mL) of the **CC3**-*R*/**CC3**-*S* racemate.

POCs with different geometries have divergent physical properties,[7, 15] which results from their different crystal packings and the impact of this on pore connectivity, internal cavity size, window configuration, surface area, and porosity. However, it is rare to be able to study two cages with identical chemical composition, but different geometries. Here, we can identify differences that arise purely from the *shape* of the cage molecules. We therefore investigated the solid-state crystal packing and physical properties of this new **CC3**-*RS*/**CC3**-*SR* racemate compare to the previously reported racemate, **CC3**-*R*/**CC3**-*S.*

CC3-*RS*/**CC3**-*SR* was isolated from the reaction mixture in solution by filtration to remove the **CC3-***R*/**CC3-***S* precipitate. The filtrate was then reduced in volume and poured into hexane, resulting in a white precipitate that was isolable by filtration. Unlike **CC3-***R*/**CC3-***S* (solubility of < 1 mg/mL in $CHCl_3$), and to a lesser extent **CC3**-*R* (solubility of 3 mg/mL),[22] the solid product was highly soluble in chloroform (48 mg/mL, **SI Section 1**). The solid **CC3-***RS*/**CC3-***SR* precipitate was found to be crystalline and easily distinguished from **CC3-***R*/**CC3-***S* by PXRD (**Fig 4biii** and **ii,** blue and red line respectively, **SI Section 2.9**). Single crystals of the filtrate were grown from DCM/hexane, DCM/acetone, and DCM/MeOH by vial-in-vial crystallisation experiments. Single crystal X-ray diffraction (SCXRD) unambiguously identified the product as a racemate of **CC3**-*RS* and **CC3**-*SR* which has crystallised in the trigonal space group *R*-3 (**Fig 4a, SI Section 2.8**) and the simulated PXRD diffraction pattern of the crystal structure matches with the PXRD pattern of the hexane precipitated filtrate (**Fig 4biii** and **iv**, pink and blue line respectively). **CC3-***RS* and **CC3-***SR* both have one triangular window with an equilateral shape, identical to the windows found in **CC3**-*R* (or -*S*). However, unlike **CC3**-*R* (or -*S*), in **CC3-***RS* and **CC3-***SR* there are three windows with an acute triangle shape. In addition, one aromatic ring is angled towards the centre of the cage cavity (**SI Section 2.8**). During crystallisation, **CC3**-*RS* and **CC3**-*SR* self-sort into 1-D packed arrangements. In the structure, **CC3**-*RS* packs in an alternating window-to-window and arene-to-arene packing arrangement (**Fig. 4a,** central two cages). 1-D packed arrangements of **CC3**-*SR* are equivalent and related by inversion symmetry. By contrast, there are no arene-to-arene contacts in chiral **CC3** or in the previously reported racemate, **CC3-***R*/**CC3-***S*.

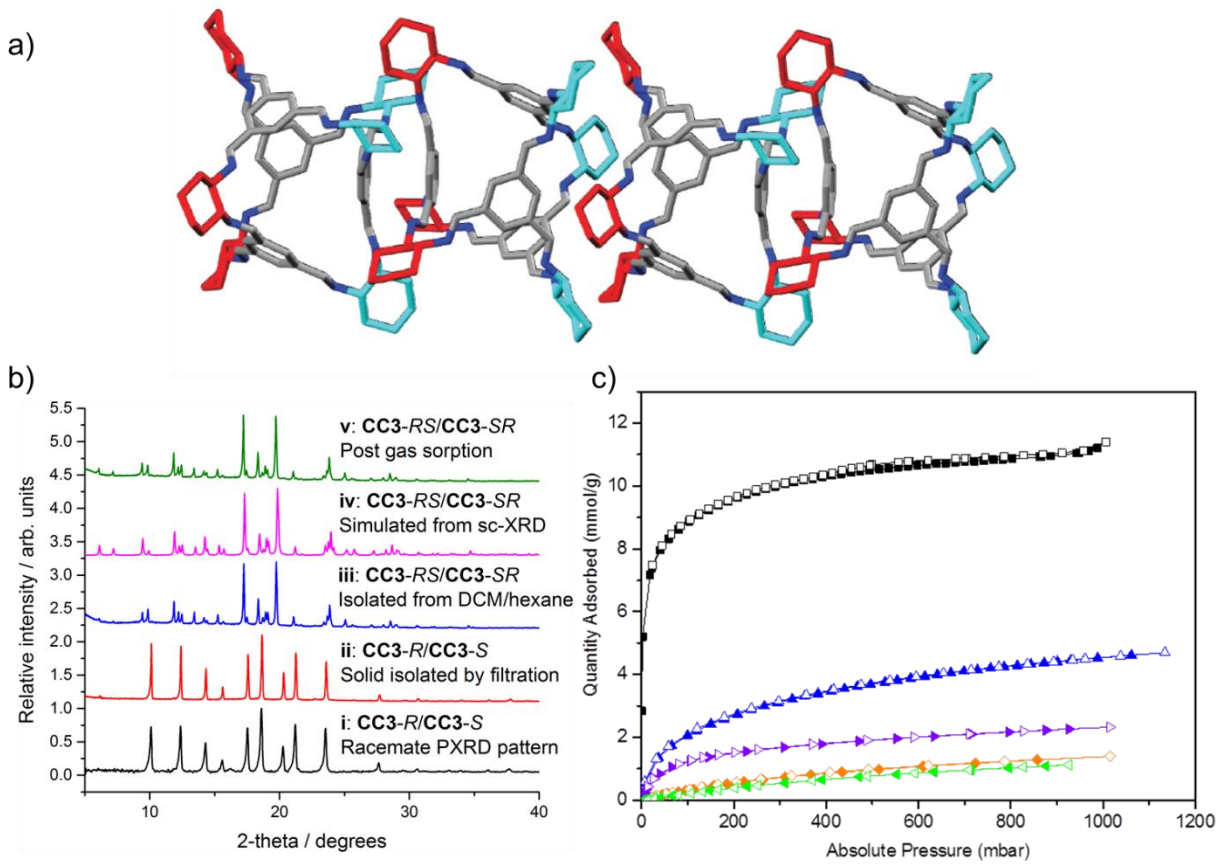

Fig 4 a) Four cages are shown with both arene-to-arene (leftmost cage pair) and window-to-window packing (central cage pair), taken from the single crystal structure of **CC3**-*RS*/**CC3**-*SR* (**SI Section 2.8**). Hydrogen atoms removed for clarity; colouring as in Fig 1. b) PXRD patterns of (i) known racemate **CC3**-*R*/**CC3**-*S*, (ii) **CC3**-*R*/**CC3**-*S* precipitate isolated via filtration; (iii) **CC3**-*RS*/**CC3**-*SR* isolated by precipitation with hexane, (iv) simulated PXRD from sc-XRD data for **CC3**-*RS*/**CC3**-*SR* and (v) **CC3**-*RS*/**CC3**-*SR* post gas sorption measurements. c) Gas sorption isotherms for **CC3**-*RS*/**CC3**-*SR* for N_2 (77 K, black), H_2 (77 K, blue), CO_2 (295 K, orange), Xe (273 K, purple), and Kr (273 K, green). Filled and open symbols represent adsorption and desorption isotherms respectively.

Gas sorption measurements (**Fig 4c**) showed **CC3**-*RS*/**CC3**-*SR* has an apparent BET surface area of 800 m^2g^{-1} (SI section 2.10), as compared to values of 409 – 819 m^2g^{-1} and up to 696 m^2g^{-1} obtained for **CC3**-*R* and **CC3-***R*/**CC3-***S*, respectively (the higher values were obtained from rapidly precipitated samples with a high proportion of structural defects).[11] As such, the dissymmetric crystalline racemate is more porous than either crystalline form of **CC3** reported so far, and its surface area is similar to that reported previously for amorphous **CC3**.[11, 23] As the **CC3**-*RS*/**CC3**-*SR* used for gas sorption was isolated by rapid precipitation, there is likely to be a contribution to porosity from crystal defects in the sample, as seen for rapidly precipitated **CC3**.[11] As much higher concentrations of the dissymmetric cage can be achieved in solution than for **CC3**, it is likely that crystallisation conditions favouring higher defect inclusion can be achieved via rapid precipitation, potentially achieving even higher gas sorption capacities. The isolated crystalline solid is stable to > 300 °C, and it is also stable in neutral solutions in DCM for at least 6 days, thus it can be solution processed without conversion to alternative diastereomers of **CC3**.

Conclusions

A new diastereomer of the well-known homochiral POC, **CC3**, has been isolated and identified as **CC3**-*RS*. **CC3**-*RS* surpasses crystalline **CC3**-*R* and **CC3**-*R*/**CC3**-*S* in terms of both solubility and microporosity, and it does not require the use of expensive homochiral amines. An oft-cited advantage of imine condensation routes to POCs is that the reactions are one-pot in nature. This study shows, however, that the cage-forming mechanism can be more complex than implied by the majority product (Fig. 3). In turn, this suggests that it might be useful to pay more attention to *in situ* reaction monitoring for these systems in the future.

Notes and references

† Notation used throughout the text for **CC3** is as follows: **CC3**-*R* and **CC3**-*S* are enantiomerically pure cages; **CC3**-*R*/**CC3**-*S* is the racemic co-crystal of **CC3**-*R* and **CC3**-*S*; **CC3**-*RS* and **CC3**-*SR*, the new cages reported here, are a racemate pair of diastereomers of **CC3**; **CC3**-*RS*/**CC3**-*SR* refers to the co-crystal containing both **CC3**-*RS* and **CC3**-*SR*.

Conflicts of interest

There are no conflicts of interest to declare.

Acknowledgements

We acknowledge the EPSRC (EP/N004884/1) and European Research Council under the European Union's Seventh Framework Programme (FP/2007-2013) through grant agreement n. 321156 (ERC-AG-PE5-ROBOT) for funding. KEJ thanks the Royal Society for a University Research Fellowship; AGS thanks the Royal Society and the EPSRC for a Royal Society-EPSRC Dorothy Hodgkin Fellowship. The authors thank Dr Tom Hasell for useful discussions. We acknowledge Stephen Moss and the MicroBioRefinery for assistance with QTOF-MS measurements.

1. D. S. Sholl and R. P. Lively, *Nature*, 2016, **533**, 316-316.
2. M. Mulder, *Basic principles of membrane technology*, Kluwer Academic, Dordrecht ; Boston, 2nd edn., 1996.
3. M. Mastalerz, *Angew Chem Int Ed*, 2010, **49**, 5042-5053.
4. L. Chen, P. S. Reiss, S. Y. Chong, D. Holden, K. E. Jelfs, T. Hasell, M. A. Little, A. Kewley, M. E. Briggs, A. Stephenson, K. M. Thomas, J. A. Armstrong, J. Bell, J. Busto, R. Noel, J. Liu, D. M. Strachan, P. K. Thallapally and A. I. Cooper, *Nat Mater*, 2014, **13**, 954-960.
5. M. A. Little, M. E. Briggs, J. T. A. Jones, M. Schmidtmann, T. Hasell, S. Y. Chong, K. E. Jelfs, L. J. Chen and A. I. Cooper, *Nat Chem*, 2015, **7**, 153-159.
6. Q. Song, S. Jiang, T. Hasell, M. Liu, S. Sun, A. K. Cheetham, E. Sivaniah and A. I. Cooper, *Adv Mater*, 2016, **28**, 2629-2637.
7. T. Tozawa, J. T. A. Jones, S. I. Swamy, S. Jiang, D. J. Adams, S. Shakespeare, R. Clowes, D. Bradshaw, T. Hasell, S. Y. Chong, C. Tang, S. Thompson, J. Parker, A. Trewin, J. Bacsa, A. M. Z. Slawin, A. Steiner and A. I. Cooper, *Nat Mater*, 2009, **8**, 973-978.
8. T. Hasell, M. Miklitz, A. Stephenson, M. A. Little, S. Y. Chong, R. Clowes, L. Chen, D. Holden, G. A. Tribello, K. E. Jelfs and A. I. Cooper, *J Am Chem Soc*, 2016, **138**, 1653-1659.
9. A. Kewley, A. Stephenson, L. J. Chen, M. E. Briggs, T. Hasell and A. I. Cooper, *Chem Mater*, 2015, **27**, 3207-3210.
10. T. Mitra, K. E. Jelfs, M. Schmidtmann, A. Ahmed, S. Y. Chong, D. J. Adams and A. I. Cooper, *Nat Chem*, 2013, **5**, 276-281.
11. T. Hasell, S. Y. Chong, K. E. Jelfs, D. J. Adams and A. I. Cooper, *J Am Chem Soc*, 2012, **134**, 588-598.

12. J. T. A. Jones, T. Hasell, X. F. Wu, J. Bacsa, K. E. Jelfs, M. Schmidtmann, S. Y. Chong, D. J. Adams, A. Trewin, F. Schiffman, F. Cora, B. Slater, A. Steiner, G. M. Day and A. I. Cooper, *Nature*, 2011, **474**, 367-371.
13. T. Hasell, M. A. Little, S. Y. Chong, M. Schmidtmann, M. E. Briggs, V. Santolini, K. E. Jelfs and A. I. Cooper, *Nanoscale*, 2017, **9**, 6783-6790.
14. T. Hasell, S. Y. Chong, M. Schmidtmann, D. J. Adams and A. I. Cooper, *Angew Chem Int Ed*, 2012, **51**, 7154-7157.
15. A. G. Slater, M. A. Little, A. Pulido, S. Y. Chong, D. Holden, L. Chen, C. Morgan, X. Wu, G. Cheng, R. Clowes, M. E. Briggs, T. Hasell, K. E. Jelfs, G. M. Day and A. I. Cooper, *Nat Chem*, 2017, **9**, 17-25.
16. T. Hasell, M. Schmidtmann, C. A. Stone, M. W. Smith and A. I. Cooper, *Chem Commun*, 2012, **48**, 4689-4691.
17. M. Liu, M. A. Little, K. E. Jelfs, J. T. A. Jones, M. Schmidtmann, S. Y. Chong, T. Hasell and A. I. Cooper, *J Am Chem Soc*, 2014, **136**, 7583-7586.
18. http://www.sigmaaldrich.com/catalog/search?interface=All&term=cyclohexanediamine&N=0&focus=product&lang=en&region=GB accessed on 7th August 2017
19. G. Zhu, C. D. Hoffman, Y. Liu, S. Bhattacharyya, U. Tumuluri, M. L. Jue, Z. Wu, D. S. Sholl, S. Nair, C. W. Jones and R. P. Lively, *Chem Eur J*, 2016, **22**, 10743-10747.
20. S. Jiang, J. T. Jones, T. Hasell, C. E. Blythe, D. J. Adams, A. Trewin and A. I. Cooper, *Nat Commun*, 2011, **2**, 207.
21. D. Beaudoin, F. Rominger and M. Mastalerz, *Angew Chem Int Ed Engl*, 2017, **56**, 1244-1248.
22. R. L. Greenaway, D. Holden, E. G. B. Eden, A. Stephenson, C. W. Yong, M. J. Bennison, T. Hasell, M. E. Briggs, S. L. James and A. I. Cooper, *Chem Sci*, 2017, **8**, 2640-2651.
23. S. Jiang, K. E. Jelfs, D. Holden, T. Hasell, S. Y. Chong, M. Haranczyk, A. Trewin and A. I. Cooper, *J Am Chem Soc*, 2013, **135**, 17818-17830.